

Supplement of Earth Syst. Dynam., 5, 423–439, 2014
<http://www.earth-syst-dynam.net/5/423/2014/>
doi:10.5194/esd-5-423-2014-supplement
© Author(s) 2014. CC Attribution 3.0 License.



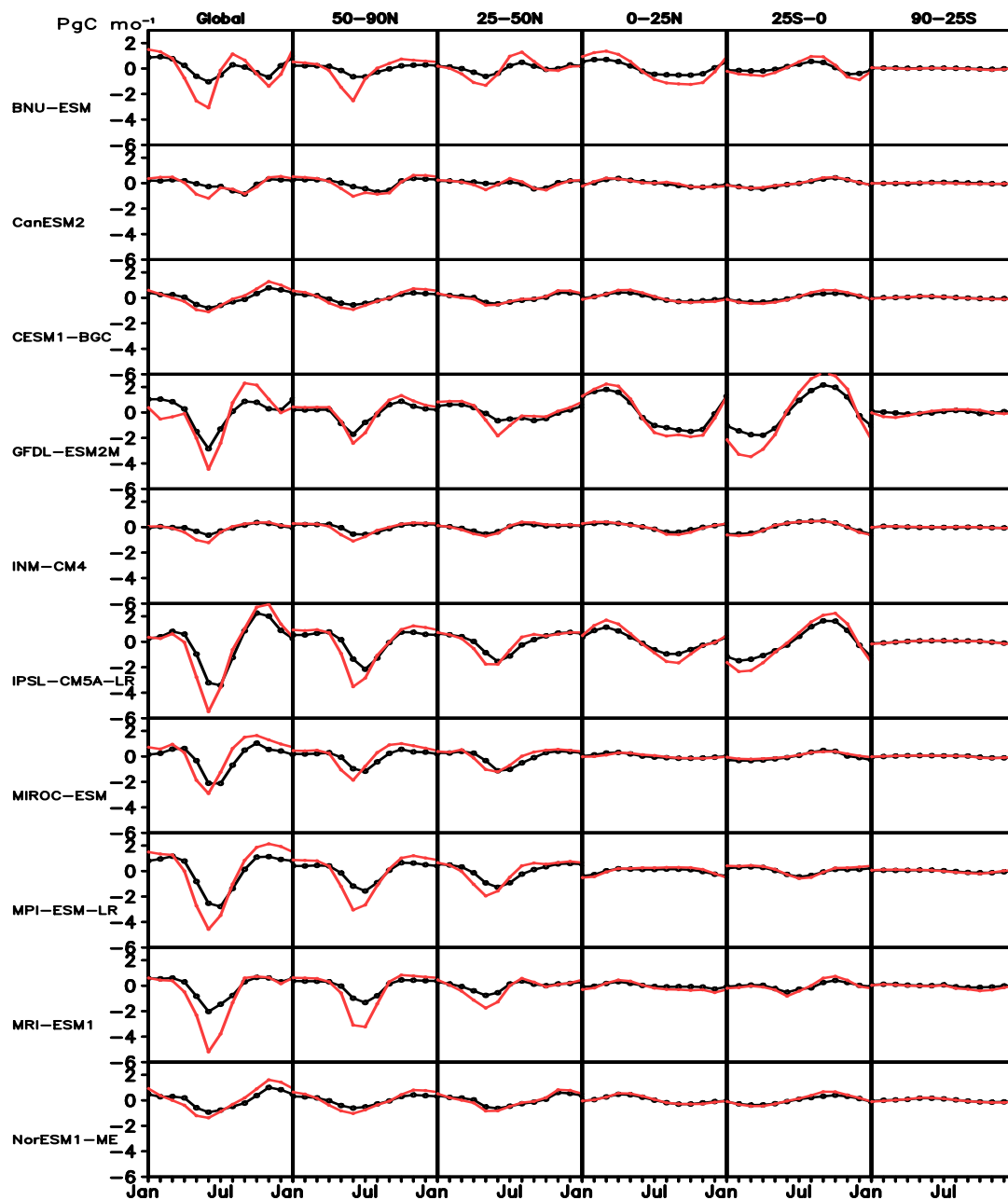
Supplement of

Continued increase in atmospheric CO₂ seasonal amplitude in the 21st century projected by the CMIP5 Earth system models

F. Zhao and N. Zeng

Correspondence to: N. Zeng (zeng@atmos.umd.edu)

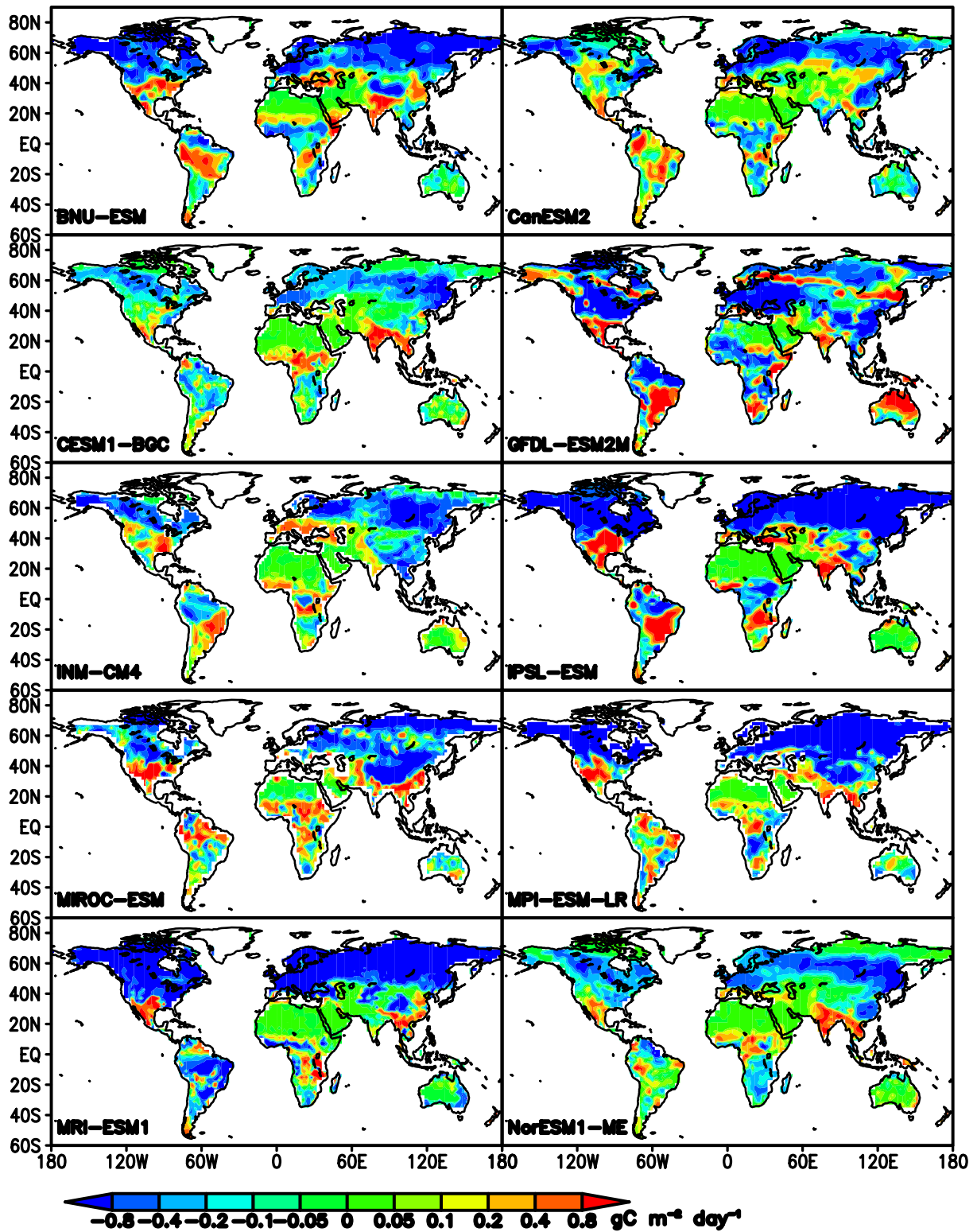
1 Supplemental Figures



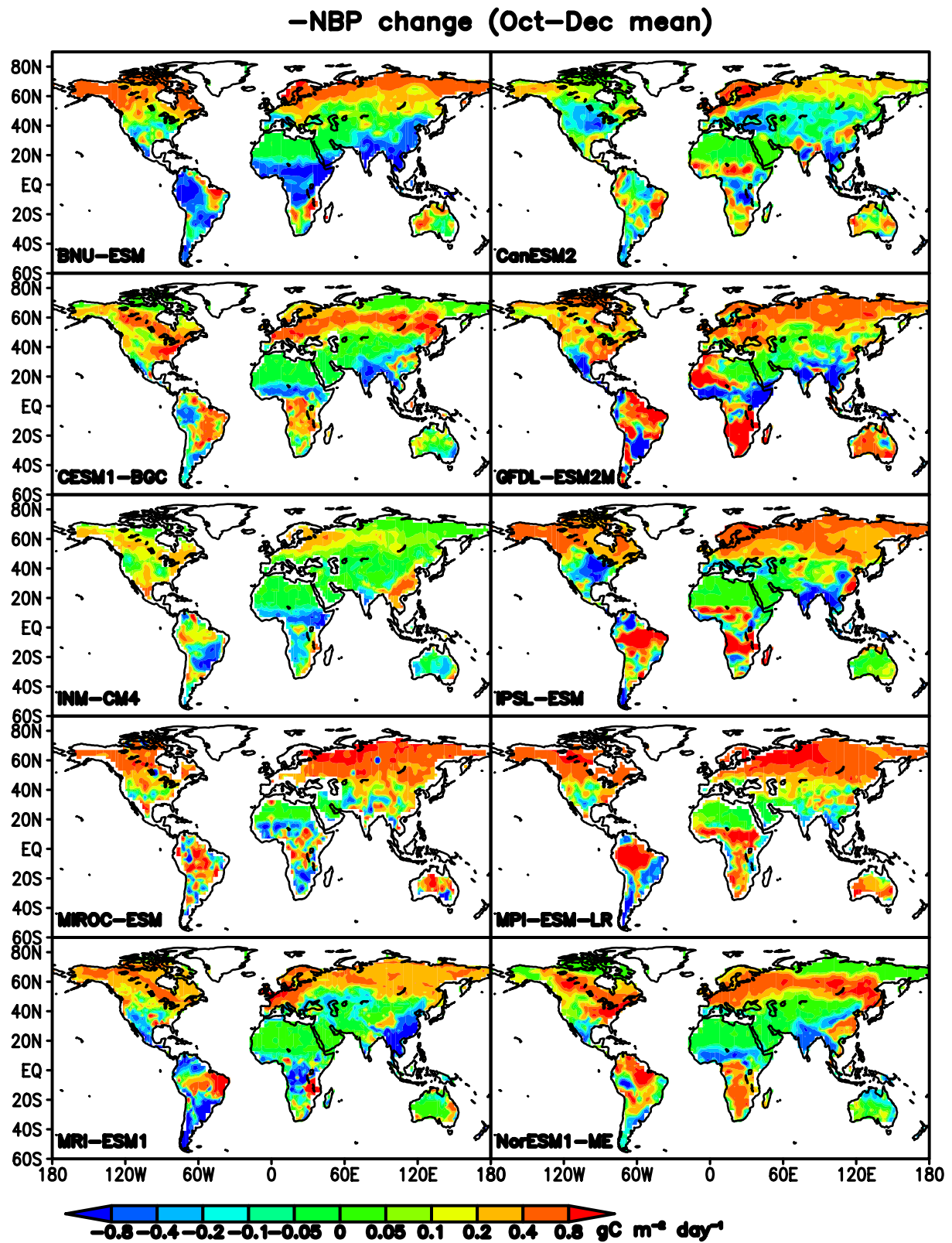
2

3 Figure S1. Seasonal cycles of global and regional total $-NBP$, averaged over 1961-1970
 4 (black) and 2081-2090 (red). The last month of the year is repeated. The Northern and
 5 Southern subtropics are clearly out of phase and largely cancel each other out. GFDL-
 6 ESM2M represents the largest tropical contribution to its global $-NBP$ seasonal cycle
 7 (maxima in September and minima in June) of all models, accounting for about a quarter of
 8 the amplitude increase.

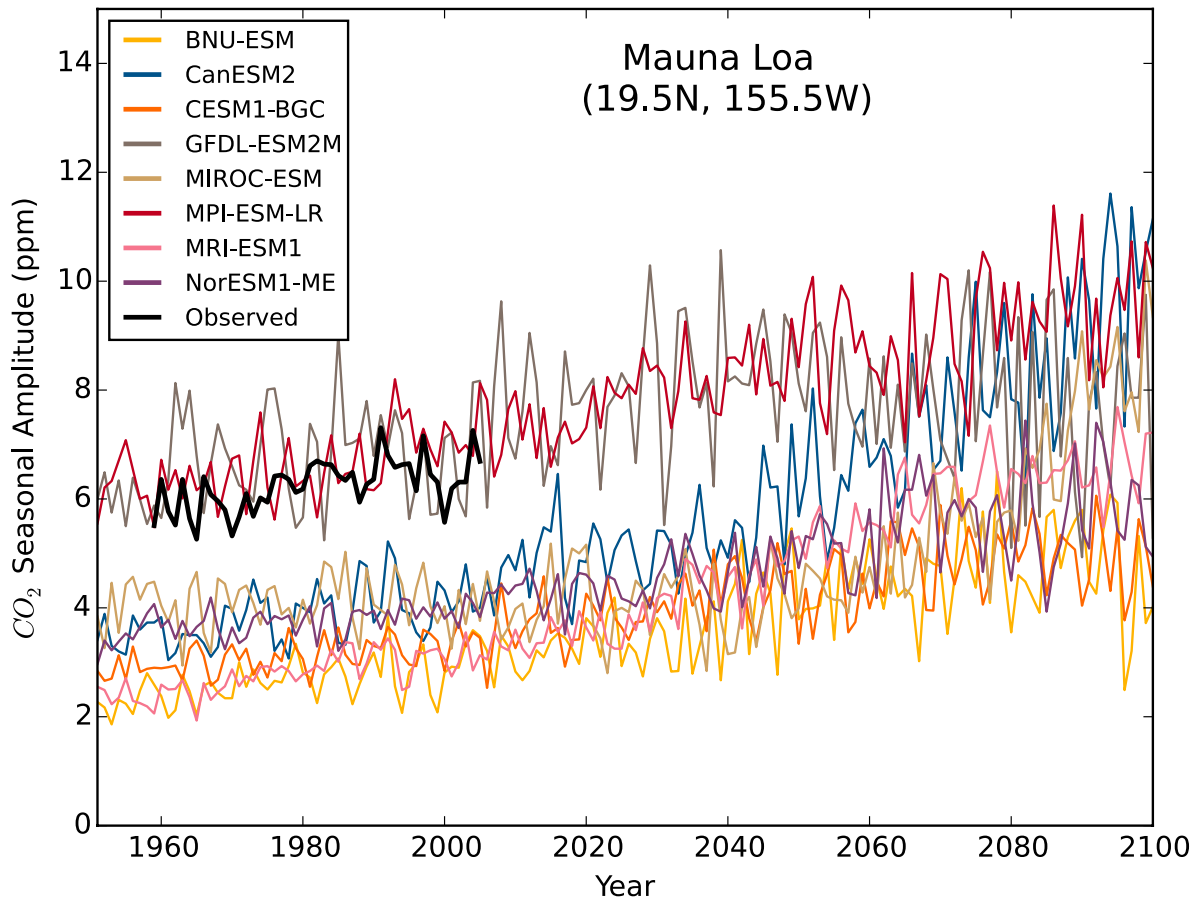
-NBP change (May-Jul mean)



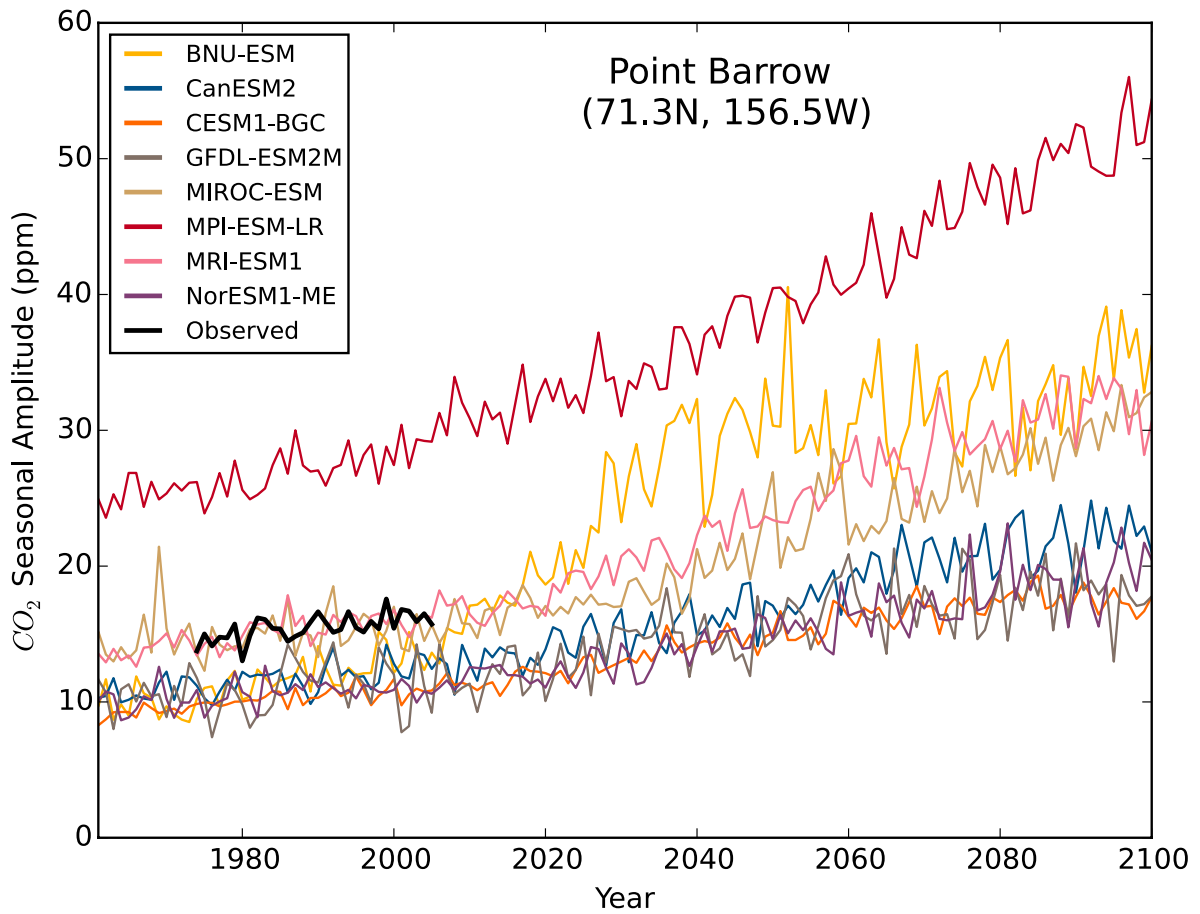
1 Figure S2. Spatial patterns of $-NBP$ ($\text{gC m}^{-2} \text{day}^{-1}$) changes between 2081-2090 and 1961-
2 1970, during peak growing season (May-July mean) for the 10 models.



1 Figure S3. Spatial patterns of $-NBP$ ($\text{gC m}^{-2} \text{ day}^{-1}$) changes between 2081-2090 and 1961-
 2 1970, during dormant season (October-December mean) for the 10 models.

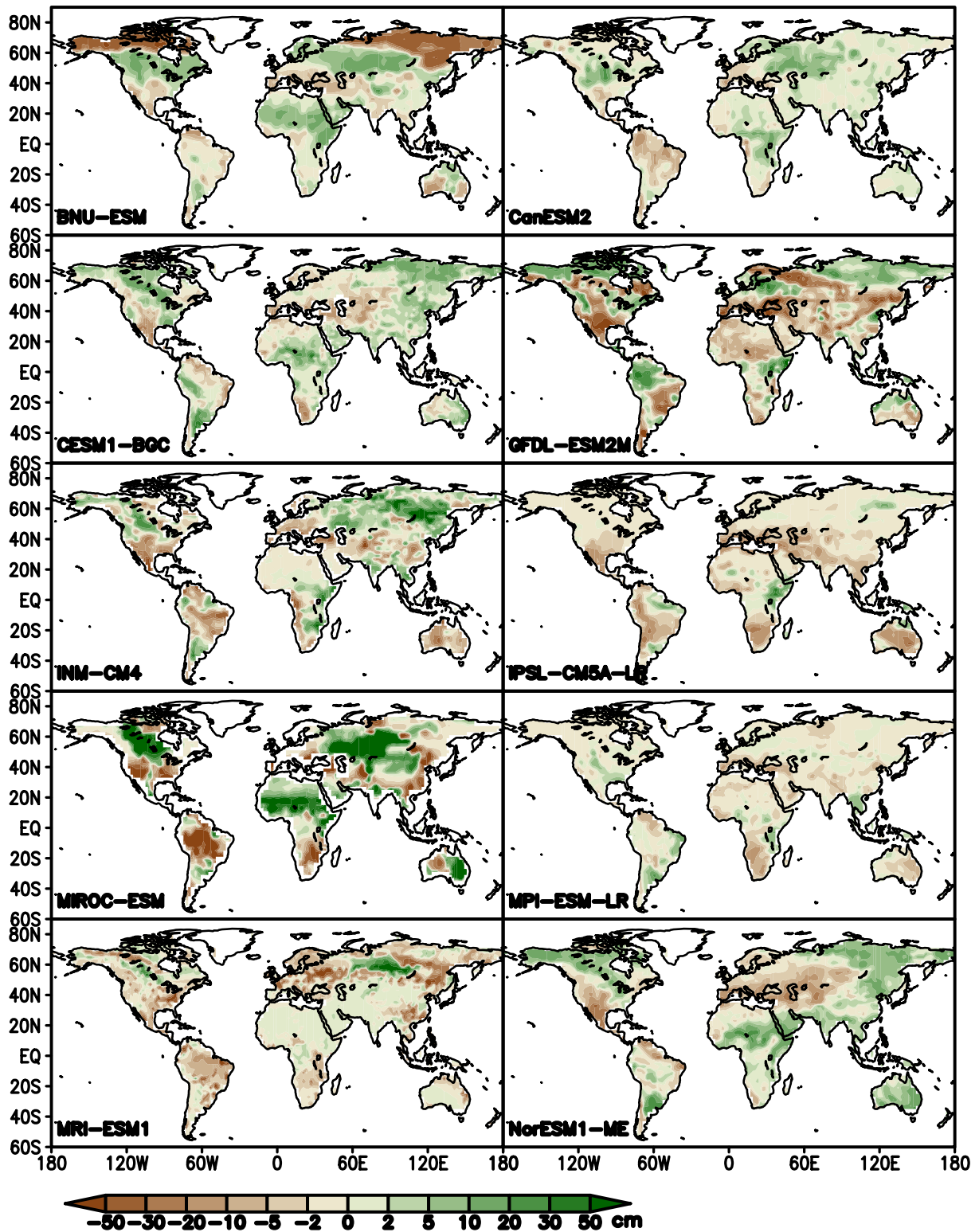


1
 2 Figure S4. CO₂ seasonal amplitude (1951-2100) from eight models (excluding INM and
 3 IPSL) at the model grid that covers Mauna Loa, Hawaii (19.5°N, 155.6°W) at 700hPa. The
 4 thick black line represents seasonal amplitude of observed Mauna Loa CO₂ records during
 5 1959-2005. All curves are computed by the CCGCRV package. Note that 1951-2005 model
 6 data are from esmHistorical, and 2006-2100 data are from esmRCP85.



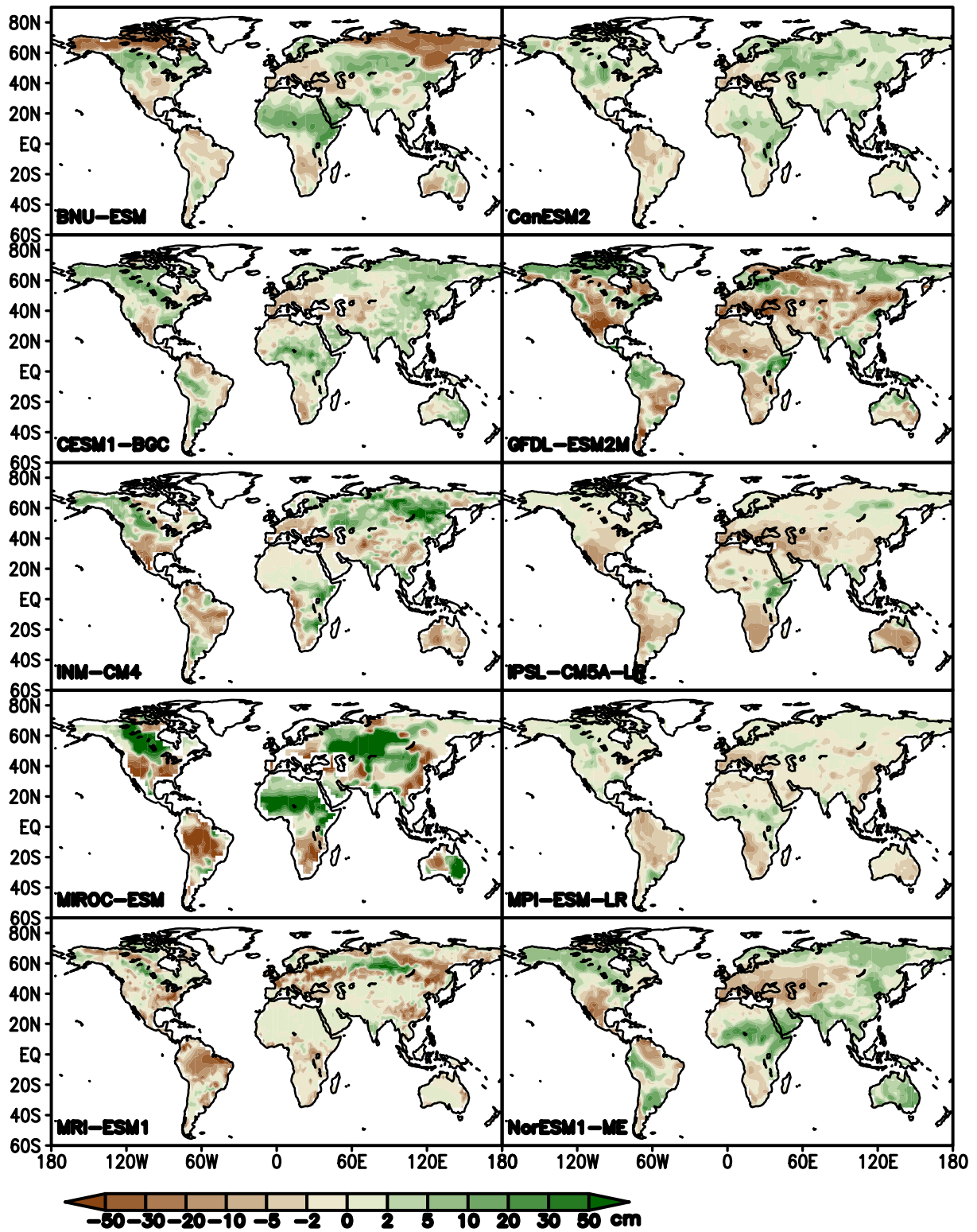
1
 2 Figure S5. CO_2 seasonal amplitude (1951-2100) from 8 models (excluding INM and IPSL) at
 3 the model grid that covers Point Barrow, Alaska (71.3N, 156.5W) at lowest level (four
 4 models at 1000hPa, and four others at 925hPa). The thick black line represents seasonal
 5 amplitude of observed Point Barrow CO_2 records during 1974-2005. All curves are computed
 6 by the CCGCRV package. Note that 1951-2005 model data are from esmHistorical, and
 7 2006-2100 data are from esmRCP85.

Soil Moisture change (May–Jul mean)



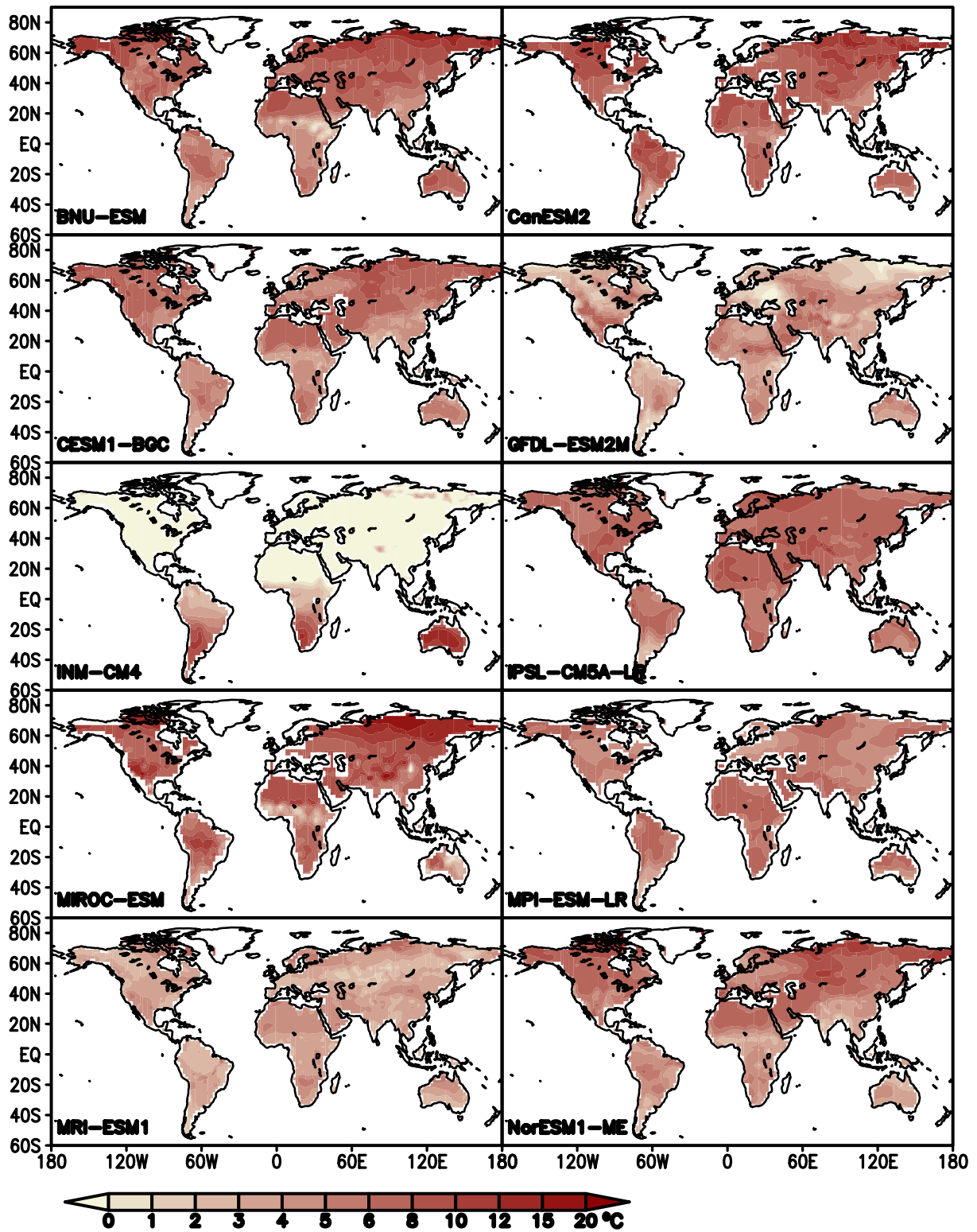
1 Figure S6. Spatial patterns of soil moisture (cm) changes between 2081-2090 and 1961-1970,
 2 during peak growing season (May–July mean) for the 10 models.

Soil Moisture change (Oct-Dec mean)



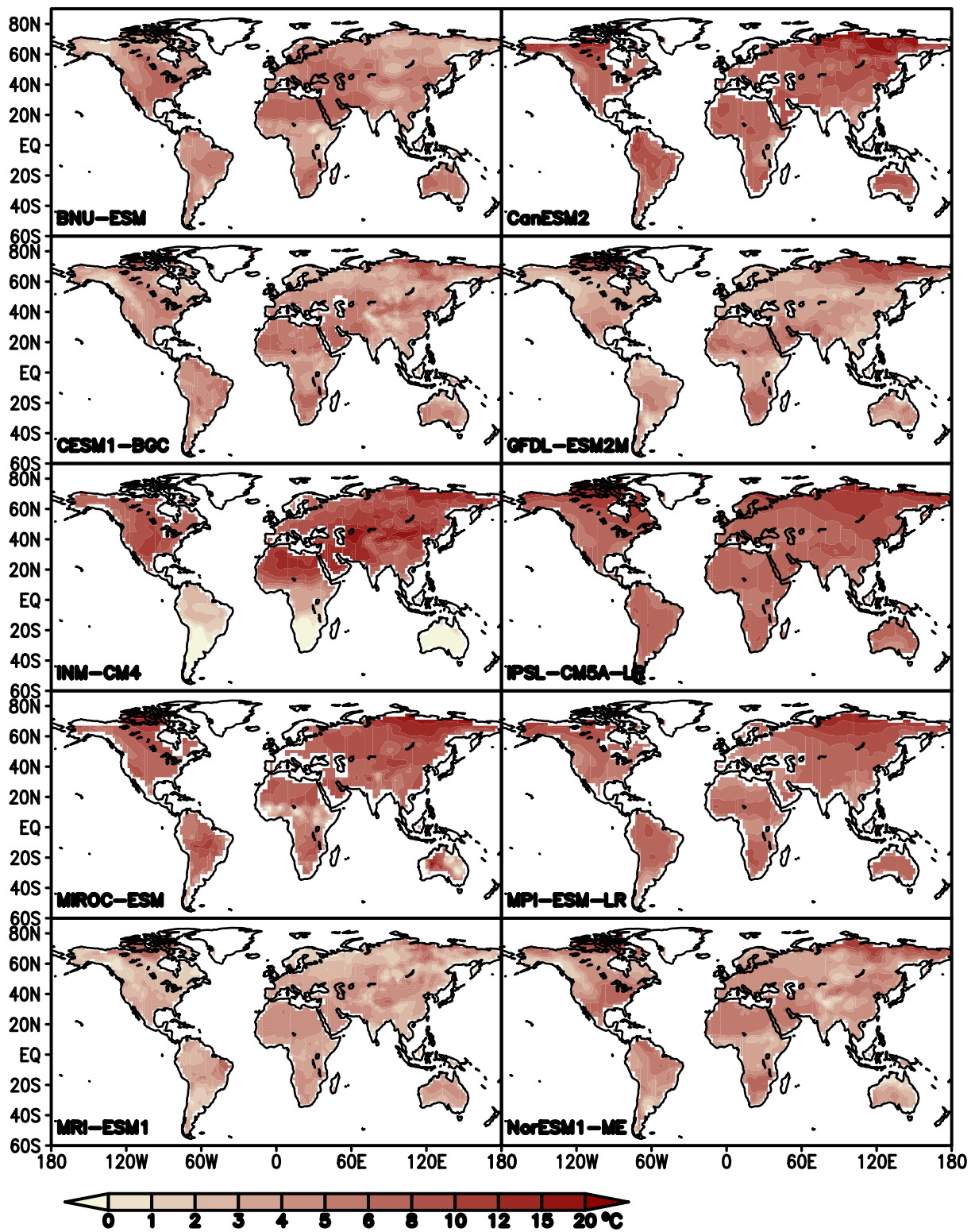
1 Figure S7. Spatial patterns of soil moisture (cm) changes between 2081-2090 and 1961-1970,
2 during dormant season (October-December mean) for the 10 models.

Near-Surface Soil Temperature change (May-Jul mean)



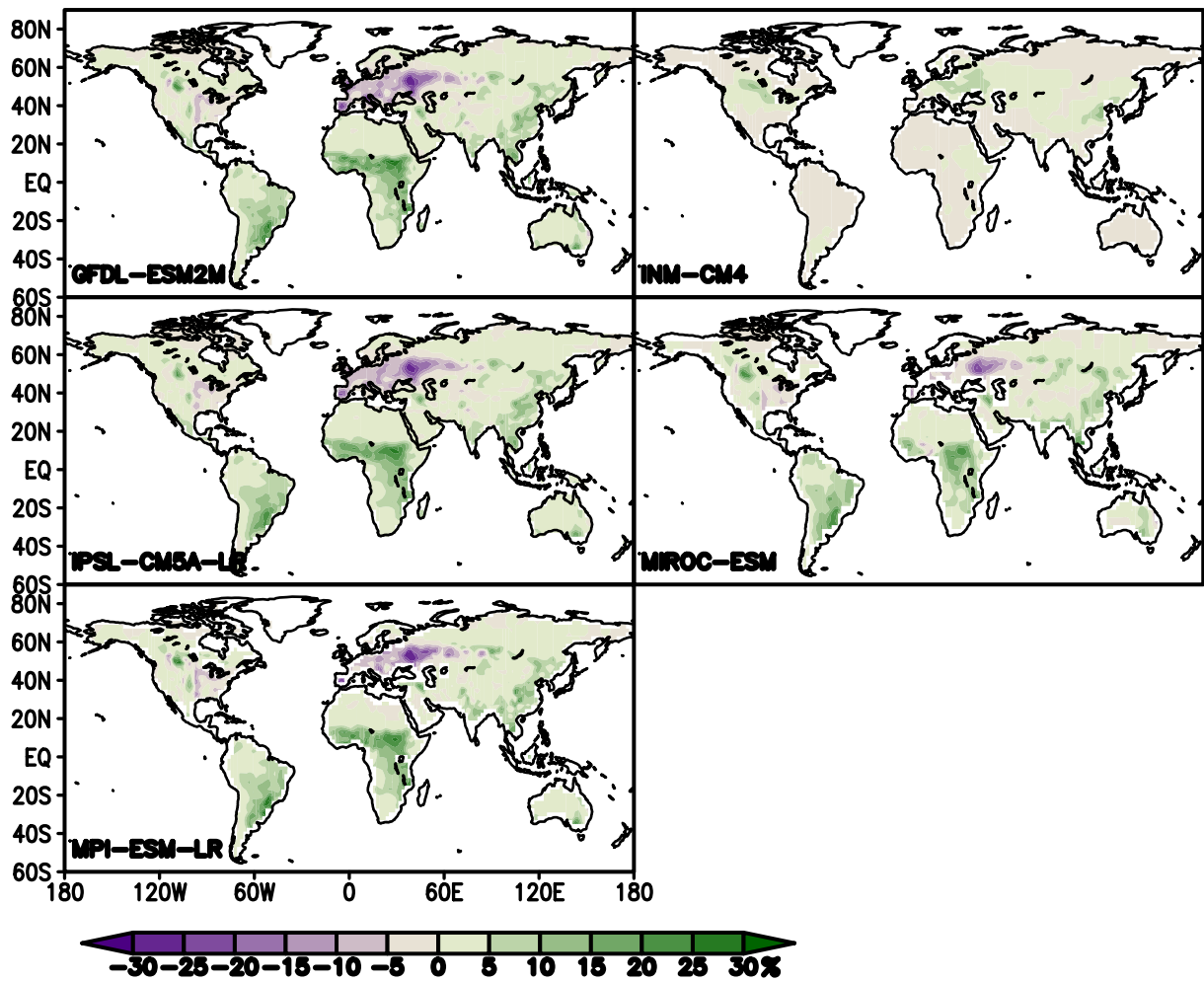
1 Figure S8. Spatial patterns of near-surface soil temperature ($^{\circ}\text{C}$) changes between 2081-2090
 2 and 1961-1970, during peak growing season (May-July mean) for the 10 models.

Near-Surface Soil Temperature change (Oct-Dec mean)



1 Figure S9. Spatial patterns of near-surface soil temperature ($^{\circ}\text{C}$) changes between 2081-2090
 2 and 1961-1970, during dormant season (October-December mean) for the 10 models.

Crop fraction change (2081–2090 – 1961–1970)



1 Figure S10. Changes of crop fraction between future (2081-2090) and historical (1961-1970)
2 periods for five CMIP5 ESMs. Except for INM-CM4, the models show similar patterns of
3 crop fraction change, which is expected given they are all driven by the same land cover
4 change scenario.

5